Mon. Not. R. Astron. Soc. **377,** 1711–1716 (2007) doi:10.1111/j.1365-2966.2007.11734.x

The imprint of massive black hole formation models on the *LISA* data stream

Alberto Sesana,[1⋆] Marta Volonteri[2,3] and Francesco Haardt[1]

[1]*Dipartimento di Fisica & Matematica, Universitá dell'Insubria, via Valleggio 11, 22100 Como, Italy*
[2]*Department of Physics and Astronomy, Northwestern University, 2145 Sheridan Avenue, Evanston, IL, USA*
[3]*Department of Astronomy, University of Michigan, 500 Church Street, Ann Arbor, MI, USA*

Accepted 2007 March 12. Received 2007 March 12; in original form 2006 December 12

ABSTRACT

The formation, merging and accretion history of massive black holes (MBHs) along the hierarchical build-up of cosmic structures leaves a unique imprint on the background of gravitational waves (GWs) at mHz frequencies. We study here, by means of dedicated simulations of black hole build-up, the possibility of constraining different models of black hole cosmic evolution using future GW space-borne missions, such as *LISA*. We consider two main scenarios for black hole formation, namely, one where seeds are light ($\simeq 10^2\,\mathrm{M}_\odot$, remnant of Population III stars) and one where seeds are heavy ($\gtrsim 10^4\,\mathrm{M}_\odot$, direct collapse). In all the models we have investigated, MBH binary coalescences do not produce a stochastic GW background, but rather, a set of individual resolved events. Detection of several hundreds merging events in a 3-yr *LISA* mission will be the sign of a heavy seed scenario with efficient formation of black hole seeds in a large fraction of high-redshift haloes. At the other extreme, a low event rate, about a few tens in 3 yr, is peculiar of scenarios where either the seeds are light, and many coalescences do not fall into the *LISA* band, or seeds are massive, but rare. In this case a decisive diagnostic is provided by the shape of the mass distribution of detected events. Light binaries ($m < 10^4\,\mathrm{M}_\odot$) are predicted in a fairly large number in Population III remnant models, but are totally absent in direct collapse models. Finally, a further, helpful diagnostic of black hole formation models lies in the distribution of the mass ratios in binary coalescences. While heavy seed models predict that most of the detected events involve equal-mass binaries, in the case of light seeds, mass ratios are equally distributed in the range 0.1–1.

Key words: black hole physics – gravitational waves – cosmology: theory – early Universe.

1 INTRODUCTION

Massive black hole (MBH) binaries (MBHBs) are among the primary candidate sources of gravitational waves (GWs) at mHz frequencies (see e.g. Haehnelt 1994; Jaffe & Backer 2003; Wyithe & Loeb 2003; Sesana et al. 2004, 2005), the range probed by the space-based *Laser Interferometer Space Antenna* (*LISA*, Bender et al. 1994). Today, MBHs are ubiquitous in the nuclei of nearby galaxies (see e.g. Magorrian et al. 1998). If MBHs were also common in the past (as implied by the notion that many distant galaxies harbour active nuclei for a short period of their life), and if their host galaxies experience multiple mergers during their lifetime, as dictated by popular cold dark matter (CDM) hierarchical cosmologies, then MBHBs inevitably formed in large numbers during cosmic history. MBHBs that are able to coalesce in less than a Hubble time (as defined at the epoch of their formation) give origin to the loudest GW signals in the Universe. Provided MBHBs do not 'stall', their GW driven inspiral will then follow the merger of galaxies and proto-galactic structures at high redshifts. A low-frequency detector like *LISA* will be sensitive to GWs from coalescing binaries with total masses in the range 10^3–$10^6\,\mathrm{M}_\odot$ out to $z \sim 5$–10 (Hughes 2002). Two outstanding questions are then how far up in the dark halo merger hierarchy do MBHs form, and whether stellar and/or gas dynamical processes can efficiently drive wide MBHBs to the GW emission stage.

Today we know that MBHs must have been formed early in the history of the Universe. Indeed, the luminous $z \approx 6$ quasars discovered in the Sloan Digital Sky Survey (Fan et al. 2001) imply that black holes more massive than a few billion solar masses were already assembled when the Universe was less than a billion years old. Several scenarios have been proposed for the seed MBH formation: seeds of $m_{\rm seed} \sim$ few times $100\,\mathrm{M}_\odot$ can form as remnants of metal free (Population III) stars at redshift $\gtrsim$20 (Volonteri, Haardt & Haardt 2003a, hereafter VHM), while intermediate-mass seeds ($m_{\rm seed} \sim 10^5\,\mathrm{M}_\odot$) can be the end product of the dynamical

⋆E-mail: as@star.sr.bham.ac.uk

instabilities arising in massive gaseous protogalactic discs in the redshift range $10 \lesssim z \lesssim 15$ (Koushiappas, Bullock & Dekel 2004, hereafter KBD; Begelman, Volonteri & Rees 2006, hereafter BVR; Lodato & Natarajan 2006). All these models have proved successful in reproducing the active galactic nucleus (AGN) optical luminosity function (LF) in a large redshift range ($1 \lesssim z \lesssim 6$), but result in different coalescence rates of MBHBs, and hence in different GW backgrounds.

In this paper we use the computational tools developed in (Sesana et al. 2005), to characterize the expected GW signal from inspiralling MBHBs in the different seed formation scenarios. Our aim is to understand the *LISA* capability to place constraints on MBH formation scenarios prior to the reionization epoch, looking for reliable diagnostics to discriminate between the different models.

The paper is organized as follows. In Section 2 we describe the different proposed seed formation scenarios. In Section 3 we summarize the basic of the detection of GW from MBHBs. In Section 4 we compare the *LISA* detection rate and the properties of the detected MBHB population arising from the different seed formation scenarios. Finally, we summarize our main results in Section 5. Unless otherwise stated, all results shown below refer to the currently favoured ΛCDM world model with $\Omega_{\rm M} = 0.3, \Omega_\Lambda = 0.7, h = 0.7$, $\Omega_{\rm b} = 0.045, \sigma_8 = 0.93$ and $n = 1$.

2 MODELS OF BLACK HOLE FORMATION

In our hierarchical framework MBHs grow starting from pregalactic seed MBHs formed at early times. The merger process would inevitably form a large number of MBHBs during cosmic history. Nuclear activity is triggered by halo mergers: in each major merger the more massive hole accretes gas until its mass scales with the fifth power of the circular velocity of the host halo, normalized to reproduce the observed local correlation between MBH mass and velocity dispersion ($m_{\rm BH}$–σ_* relation). Gas accretion on to the MBHs is assumed to occur at a fraction of the Eddington rate, as empirically shown in simulations of AGN feedback in a merger driven scenario. The scaling we adopt is based on the fitting formula by Hopkins et al. (2005) (see Volonteri, Salvaterra & Salvaterra 2006, for details).

In this scenario there is a certain freedom in the choice of the seed masses, in the accretion prescription, and in the MBHB coalescence efficiency.

In the VHM model, seed MBHs form with masses $m_{\rm seed} \sim$ few times $10^2\,{\rm M}_\odot$, in haloes collapsing at $z = 20$ from rare 3.5σ peaks of the primordial density field (Madau & Rees 2001), and are thought to be the end product of the first generation of stars.

A different class of models assumes that MBH seeds form already massive. In the KBD model, seed MBHs form from the low angular momentum tail of material in haloes with efficient molecular hydrogen gas cooling. MBHs with mass

$$m_{\rm seed} \simeq 5 \times 10^4\,{\rm M}_\odot \left(\frac{M_{\rm H}}{10^7\,{\rm M}_\odot}\right)\left(\frac{1+z}{18}\right)^{3/2}\left(\frac{\lambda}{0.04}\right)^{3/2} \quad (1)$$

form in DM haloes with mass

$$M_{\rm H} \gtrsim 10^7\,{\rm M}_\odot \left(\frac{1+z}{18}\right)^{-3/2}\left(\frac{\lambda}{0.04}\right)^{-3/2}. \quad (2)$$

We have fixed the free parameters in equation (1) by requiring an acceptable match with the LF of quasars at $z < 6$. We note that, by requiring that the model reproduces the LF, the number of MBH seeds is very much reduced with respect to Koushiappas & Zentner (2006), where most of the black hole growth was due to black hole mergers.

Here λ is the so-called spin parameter, which is a measure of the angular momentum of a dark matter halo $\lambda \equiv J\,|E|^{1/2}/GM_{\rm H}^{5/2}$, where J, E and $M_{\rm h}$ are the total angular momentum, energy and mass of the halo. The angular momentum of galaxies is believed to have been acquired by tidal torques due to interactions with neighbouring haloes. The distribution of spin parameters found in numerical simulations is well fit by a lognormal distribution in $\lambda_{\rm spin}$, with mean $\bar{\lambda}_{\rm spin} = 0.04$ and standard deviation $\sigma_\lambda = 0.5$ (Bullock et al. 2001; van den Bosch et al. 2002). We have assumed that the MBH formation process proceeds until $z \approx 15$.

In the BVR model, black hole seeds form in haloes subject to runaway gravitational instabilities. Gravitational instabilities are likely the most effective process for removing angular momentum. BVR have suggested that gas-rich haloes with efficient cooling and low angular momentum (i.e. low-spin parameter) are prone to global dynamical instabilities, the so-called 'bars within bars' mechanism (Shlosman, Frank & Begelman 1989). In metal-free haloes with virial temperatures $T_{\rm vir} \gtrsim 10^4$ K, hydrogen atomic line emission can cool the gas down to ∼8000 K. In smaller haloes, provided that molecular hydrogen cooling is efficient, gas can cool well below the virial temperature. The amount of material participating in the 'bars within bars' instability, however, is much smaller in such minihaloes, leading to the accumulation in the protogalaxy centre of only a few tens of solar masses. We assumed here, as in BVR, that MBH seed formation is efficient only in metal free haloes with virial temperatures $T_{\rm vir} \gtrsim 10^4$ K. The 'bars within bars' process produces in the centre of the halo a 'quasi-star' (QSS) with a very low specific entropy. When the QSS core collapses, it leads to a seed black hole of a few tens of solar masses. Accretion from the QSS envelope surrounding the collapsed core can however build up a substantial black hole mass very rapidly until it reaches a mass of the order of the 'quasi-star' itself, $M_{\rm QSS} \simeq 10^4$–$10^5\,{\rm M}_\odot$. The black hole accretion rate adjusts so that the feedback energy flux equals the Eddington limit for the quasi-star mass; thus, the black hole grows at a super-Eddington rate as long as $M_{QSS} > M_{\rm BH}\, M_{\rm BH}(t) \sim 4 \times 10^5\,(t/10^7\,{\rm yr})^2\,{\rm M}_\odot$, that is, $M_{\rm BH} \propto t^2$.

In metal rich haloes star formation becomes efficient, and depletes the gas inflow before the conditions for QSS (and MBH) formation are reached. BVR envisage that the process of MBH formation stops when gas is sufficiently metal enriched. Given the uncertainties in the efficiency of spreading metals, we consider here two scenarios, one in which star formation exerts a high level of feedback and ensures a rapid metal enrichment (BVRhf) and one in which feedback is milder and haloes remain metal free for longer (BVRlf). In the former case MBH formation ceases at $z \approx 15$, in the latter at $z \approx 18$. The BVRhf model appears to produce barely enough MBHs to reproduce the observational constraints (ubiquity of MBHs in the local universe, LF of quasars). We consider it a very strong lower limit to the number of seeds that need to be formed in order to fit the observational constraints.

Fig. 1 shows the number of MBH binary coalescences per unit redshift per unit *observed* year, $\mathrm{d}N/\mathrm{d}z\,\mathrm{d}t$, predicted by the five models we tested. Each panel shows the rates for different $m_{\rm BH} = m_1 + m_2$ mass intervals. The total coalescence rate spans almost two orders of magnitude ranging from ∼3 yr^{-1} (BVRhf) to ∼250 yr^{-1} (KBD). As a general trend, coalescences of more massive MBHBs peak at lower redshifts (for all the models the coalescence peak in the case $m_{\rm BH} > 10^6\,{\rm M}_\odot$ is at $z \sim 2$). Note that there are no merging MBHBs with $m_{\rm BH} < 10^4\,{\rm M}_\odot$ in the KBD and BVR models.

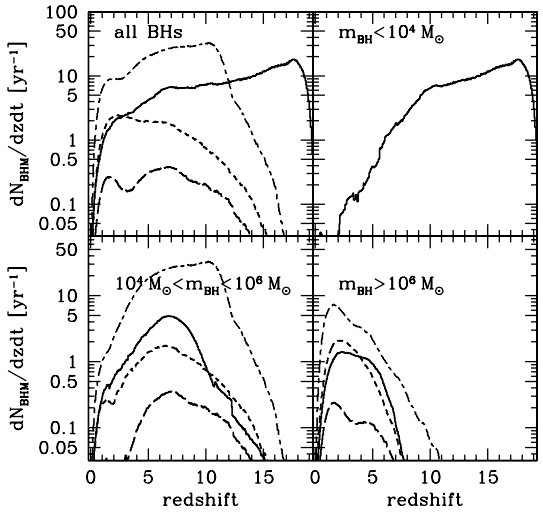

Figure 1. Number of MBHB coalescences per observed year at $z = 0$, per unit redshift, in different $m_{\rm BH} = m_1 + m_2$ mass intervals. Solid lines: VHM model; short–long-dashed lines: KBD model; short-dashed lines: BVRlf model; long-dashed lines: BVRhf model.

2.1 MBHB dynamics

During a galactic merger, the central MBHs initially share their fate with the host galaxy. The merging is driven by dynamical friction, which has been shown to efficiently merge the galaxies and drive the MBHs in the central regions of the newly formed galaxy when the mass ratio of the satellite halo to the main halo is sufficiently large, that is when (total) mass ratio of the progenitor haloes is, $P = M_{\rm s}/M \gtrsim 0.1$ (Kazantzidis et al. 2005).

The efficiency of dynamical friction decays when the MBHs get close and form a binary. In gas-poor systems, the subsequent evolution of the binary may be largely determined by three-body interactions with background stars (Begelman, Blandford & Rees 1980), leading to a long coalescence time-scale. In gas rich high-redshift haloes, the orbital evolution of the central supermassive black hole is likely dominated by dynamical friction against the surrounding gaseous medium. The available simulations (Escala et al. 2005; Dotti, Colpi & Haardt 2006a; Mayer et al. 2006) show that the binary can shrink to about parsec or slightly subparsec scale by dynamical friction against the gas, depending on the gas thermodynamics. We have assumed here that, if a hard MBH binary is surrounded by an accretion disc, it coalesces instantaneously owing to interaction with the gas disc. If instead there is no gas readily available, the binary will be losing orbital energy to the stars, using the scheme described in Volonteri, Madau & Madau (2003b) and Volonteri & Rees (2006).

3 GRAVITATIONAL WAVE SIGNALS

Full discussion of the GW signal produced by an inspiralling MBHB can be found in Sesana et al. (2005), along with all the relevant references. Here we just summarize the basic equations.

3.1 Characteristic strain

Consider a MBHB at (comoving) distance $r(z)$. The strain amplitude (sky and polarization averaged) at the rest-frame frequency $f_{\rm r}$ is (e.g. Thorne 1987)

$$h = \frac{8\pi^{2/3}}{10^{1/2}}\,\frac{G^{5/3}\mathcal{M}^{5/3}}{c^4 r(z)}\,f_{\rm r}^{2/3}, \tag{3}$$

where $\mathcal{M} = m_1^{3/5}m_2^{3/5}/(m_1+m_2)^{1/5}$ is the 'chirp mass' of the binary and all the other symbols have their standard meaning. The characteristic strain is defined as

$$h_{\rm c} = h\sqrt{n} \simeq \frac{1}{3^{1/2}\pi^{2/3}}\,\frac{G^{5/6}\mathcal{M}^{5/6}}{c^{3/2}r(z)}\,f_{\rm r}^{-1/6}, \tag{4}$$

where $\sqrt{n}$ is the number of cycles spent in a frequency interval $\Delta f \simeq f$. Equation (4) is valid only if the typical source shifting time (the time spent in a given $\Delta f \simeq f$ bin) is shorter than the instrumental operation time. This is almost always the case, as *LISA* would be sensitive to the signal emitted in the last 1–3 yr before the MBHB coalescence, and the operation time is expected to be $\gtrsim$3 yr.

3.2 Resolved events

An inspiralling binary is then detected if the signal-to-noise ratio (S/N) *integrated over the observation* is larger than the assumed threshold for detection. The integrated S/N is given by (e.g. Flanagan & Hughes 1998)

$$\mathrm{S/N}_{\Delta f} = \sqrt{\int_f^{f+\Delta f} \mathrm{d}\ln f' \left[\frac{h_{\rm c}(f'_{\rm r})}{h_{\rm rms}(f')}\right]^2}. \tag{5}$$

Here, $f = f_{\rm r}/(1+z)$ is the (observed) frequency emitted at time $t = 0$ of the observation, and Δf is the (observed) frequency shift during the observational time τ. Finally, $h_{\rm rms}$ is the effective rms noise of the instrument. The total *LISA* $h_{\rm rms}$ noise is obtained by adding in quadrature the instrumental rms noise (given by e.g. the Larson's online sensitivity curve generator http://www.srl.caltech.edu/shane/sensitivity) and the confusion noise from unresolved galactic (Nelemans, Yungelson & Portegies-Zwart 2001) and extragalactic (Farmer & Phinney 2003) WD–WD binaries. Given the uncertainties on the very-low-frequency *LISA* sensitivity, we adopt a pessimistic cut at 10^{-4} Hz. We will discuss later the impact of changing the low-frequency cut–off of the sensitivity curve.

Given a coalescence rate R, and the source frequency shift rate $\dot{f}$, we can derive the number of *individual* binaries resolved with $\mathrm{S/N} > s$, that is, (Sesana et al. 2005):

$$\%N_\tau(>s) = R\int_{f_{\rm min}}^{f_{\rm ISCO}} \frac{\mathrm{d}f}{\dot{f}}\,H_{\rm s}(\Delta f), \tag{6}$$

where

$$H_{\rm s}(\Delta f) = \begin{cases} 1, & \mathrm{S/N}_{\Delta f} \geqslant s, \\ 0, & \mathrm{S/N}_{\Delta f} < s. \end{cases} \tag{7}$$

In equation (6), $f_{\rm ISCO}$ is the observed frequency emitted at the Keplerian innermost stable circular orbit (ISCO), and $f_{\rm min} \ll f_{\rm ISCO}$ is the minimum observed frequency of the spiral-in phase.

4 MBH FORMATION MODELS AND THE GW SIGNAL

In this section we discuss the characteristics of the GW signal detectable by *LISA* as predicted by the different models of MBH formation and evolution discussed in section 2. All the results shown here assume a *LISA* operation time of 3 yr, a cut-off at 10^{-4} Hz in the instrumental sensitivity and a detection integrated threshold of $\mathrm{S/N} = 5$ (equation 5).

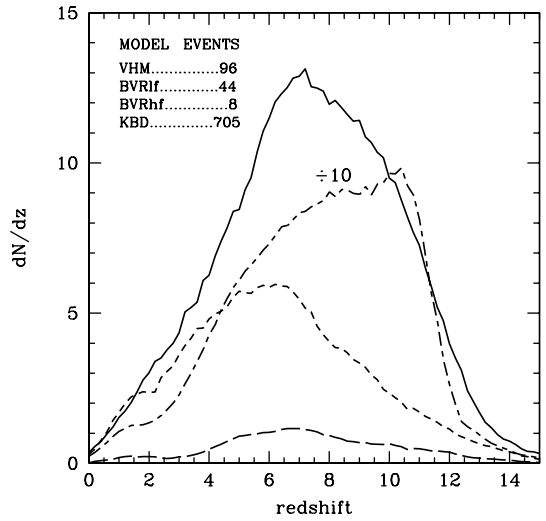

Figure 2. Redshift distribution of MBHBs resolved with S/N > 5 by *LISA* in a 3-yr mission. Line style as in Fig. 1. The number of events predicted by KBD model (long–short-dashed curve) is divided by a factor of 10. The top left-hand corner label lists the total number of expected detections.

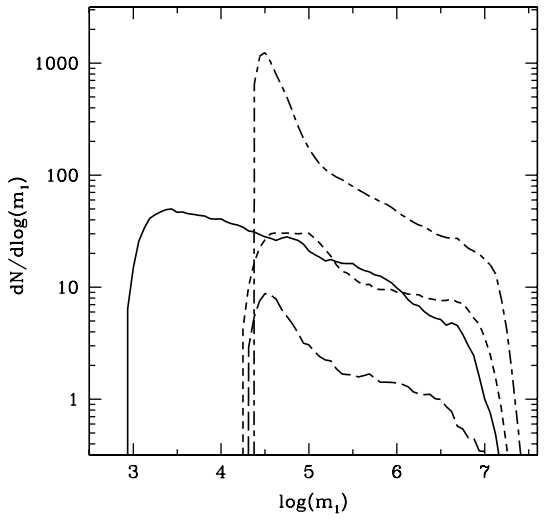

Figure 3. Mass function of the more massive member of MBHBs resolved with S/N > 5 by *LISA* in a 3-yr mission. Line style as in Fig. 1. All curves are normalized such as the integral in d log (m_1) gives the number of detected events.

4.1 Event number counts

Fig. 2 shows the redshift distribution of *LISA* MBHB detections. There are substantial differences between the different models. The KBD model results in a number of events ($\simeq$700) that is more than an order of magnitude higher than that predicted by other models, with a skewed distribution peaked at sensibly high redshift, $z \gtrsim 10$. It is interesting to compare the *number of detections* with the *total number of binary coalescences* predicted by the different formation models. The KBD model produces $\simeq$750 coalescences, the VHM model $\simeq$250 and the two BVR models just few tens. A difference of a factor of $\simeq$3 between the KBD and the VHM models in the total number of coalescences, results in a difference of a factor of $\simeq$10 in the *LISA* detections, due to the different mass of the seed black holes. Almost all the KBD coalescences involve massive binaries ($m_1 \gtrsim 10^4\,\mathrm{M}_\odot$), which are observable by *LISA*. The KBD and BVR models differ for the sheer number of MBHs. The halo mass threshold in the KBD model is well below (about three orders of magnitude) the BVR one, the latter requiring haloes with virial temperature above 10^4 K. In a broader context, results pertaining to the KBD model describe the behaviour of families of models where efficient MBH formation can happen also in minihaloes where the source of cooling is molecular hydrogen.

It is difficult, on the basis of the redshift distributions of detected binaries only, to discriminate between heavy and light MBH seed scenarios. Although the VHM and BVRlf models predict a different number of observable sources, the uncertainties in the models are so high, that a difference of a factor of 2 (96 for the VHM model, 44 for the BVRlf model) cannot be considered a safe discriminant. Moreover, the redshift distributions are quite similar, peaked at $z \simeq$ 6–7 and without any particular feature in the shape. Arguably, the initial mass distribution of seeds is the main variable influencing the number of *LISA* events. However, a factor of 2 difference in the number counts, in fact, can be ascribed to uncertainties in other aspects of the MBH evolution, both dynamical and related to the accretion history. Sesana et al. (2005) showed how uncertainties in the dynamical evolution time-scales reflect on the detectable events. Also the accretion history plays a role which may not be marginal. For instance, if MBHs grow fast (accreting around the Eddington rate or higher), the number of coalescences that can be detected by LISA is higher than, say, a case in which the accretion rate is sub-Eddington for most sources.

4.2 Black hole masses and mass ratio distributions

In Sesana et al. (2005) we showed that *LISA* will be sensitive to binaries with masses $\lesssim 10^3\,\mathrm{M}_\odot$ up to redshift 10. Hence the discrimination between heavy and light MBH seed scenarios should be easy on the basis of the mass function of detected binaries. This is shown in Fig. 3. As expected, in the VHM model, the mass distribution extends to masses $\lesssim 10^3\,\mathrm{M}_\odot$, giving a clear and unambiguous signature of a light-seed scenario. VHM predict that many detections (about 50 per cent) involve low mass binaries ($m_{\rm BH} < 10^4\,\mathrm{M}_\odot$) at high redshift ($z > 8$). These sources are observable during the inspiral phase, but their $f_{\rm ISCO}$ is too high for *LISA* detection (see Sesana et al. 2005, Fig. 2). Heavy seed scenarios predict instead that the GW emission at $f_{\rm ISCO}$, and the subsequent plunge are always observable for all binaries.

In Fig. 4 we show the mass ratio distribution of the resolved events for the VHM and the KBD models. Model KBD (as well as BVRlf and BVRhf, not shown here) predict a monotonically increasing distribution, the majority of detections having a mass ratio $q = M_2/M_1 \leqslant 1$. A large fraction of observable coalescences, in fact, involve MBHBs at $z > 10$, when MBHs had no time to accrete much mass yet. As most seeds form with similar mass ($\simeq 10^4\,\mathrm{M}_\odot$, see KBD; $\simeq 10^2\,\mathrm{M}_\odot$, see VHM), mergers at early times involve MBHBs with $q \simeq 1$. In massive seeds scenarios, almost all coalescences are observable, and the mass ratio distribution is dominated by $z > 10$ mergers between seeds ($q \simeq 1$). In scenarios based on Population III remnants, $z > 10$ mergers involve MBHs with mass below the *LISA* threshold. The detectable events happen at later times, when MBHs have already experienced a great deal of mass growth. VHM models therefore produce a mass ratio distribution which is flat or features a broad peak at $q \simeq 0.1$–0.2, depending on the details of the accretion prescription. This is due to the fact that both the probability of halo mergers (because of the steep DM halo mass function) and the dynamical friction time-scale increase with

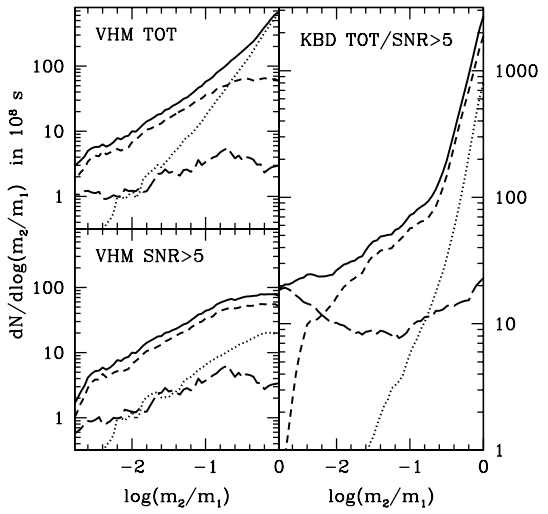

Figure 4. Mass ratio distribution of MBHBs. Long-dashed curve: $0 < z < 3$; short-dashed curve: $3 < z < 10$; dotted curve: $z > 10$; solid curve: all redshifts. Left-hand panels: VHM model, all coalescences (upper panel), and coalescences detectable by *LISA* with S/N > 5 in a 3-yr mission (lower panel). Most high-redshift events with mass ratios of the order of unity involve light binaries which cannot be observed by *LISA*. Right-hand panel: KBD model; almost all the coalescences can be observed with a S/N > 5.

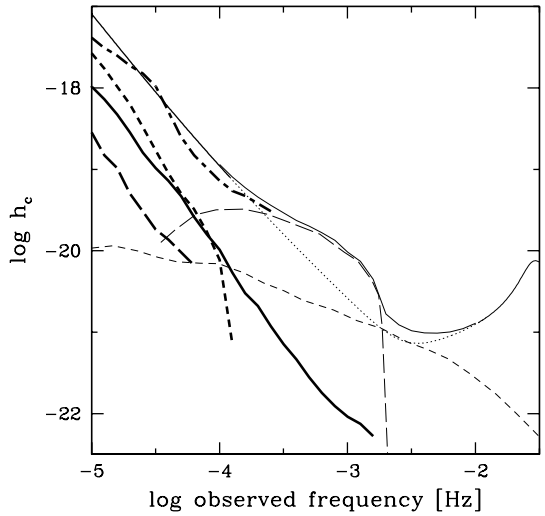

Figure 5. Predicted confusion noises assuming a *LISA* operating time of 1 yr. Thin lines: *LISA* rms confusion noise (solid line), as the quadratic sum of the *LISA* instrumental single-arm Michelson noise (dotted line, from http://www.srl.caltech.edu/∼shane/sensitivity), and the confusion noise from unresolved galactic (Nelemans et al. 2001, long-dashed line), and extragalactic (Farmer & Phinney 2003, short-dashed line) WD–WD binaries. Thick lines: predicted confusion noises for the different MBHB models we tested. Line style as in Fig. 1.

decreasing halo mass ratio. Hence, equal-mass mergers that lead to efficient binary formation within short time-scales (i.e. shorter than the Hubble time) are rare, while in more common unequal-mass mergers it takes longer than an Hubble time to drag the satellite hole to the centre.

All the results shown above assume 3-yr observation and a cut-off in the *LISA* sensitivity curve at 10^{-4} Hz. Even in the pessimistic case of a 1-yr mission lifetime, however, with a sensitivity curve cut at 10^{-4} Hz and assuming the BVRhf seed model, *LISA* is expected to observe at least two or three MBHB merging events. We stress once again that the BVRhf model provides a strong lower limit to the number and redshift distribution of forming seeds, on the basis of current observational constraints.

4.3 Confusion noise

If the number of merging sources is so large that there are, on average, at least eight sources above threshold per frequency-resolution bin, then the total signal will be observed as a confusion noise (Cornish 2003). A detectable confusion noise of cosmic origin would provide much information on the emitting population, but, on the other hand, would be added (in quadrature) to the instrumental noise, reducing the interferometer capability of detecting individual sources. Assuming a mission lifetime of 3 yr, the predicted confusion noise (see Sesana et al. 2005 for details), varies by an order of magnitude for different models, but lies, for all models, below the *LISA* sensitivity curve. In the pessimistic view of a 1-yr mission, the confusion noise is enhanced roughly by a factor of 3. As shown in Fig. 5, the confusion noise predicted by the KBD model is expected to be comparable to the rms noise at frequencies $\lesssim 3 \times 10^{-4}$ Hz. If the sensitivity curve cuts off at 10^{-5} Hz; the quadrature addition of such a noise would result in a slight decrease of the total *LISA* sensitivity in the frequency range $3 \times 10^{-5} - 3 \times 10^{-4}$ Hz.

5 SUMMARY AND CONCLUSIONS

Using dedicated Montecarlo simulations of the hierarchical assembly of DM haloes along the cosmic history, we have computed the expected GW signal from the evolving population of MBHBs. The imprint of black hole mergers and coalescences on the *LISA* data stream depends on the specific assumptions regarding MBH formation, and on the recipes employed for the hole mass growth via merger and gas accretion.

We have considered two main frameworks for MBH formation, namely, one where seeds are light ($\simeq 10^2\,M_\odot$), and one where seeds are heavy ($\gtrsim 10^4\,M_\odot$). In the former, MBH seeds form at $z \simeq 20$ with masses of few hundreds solar masses, and are though to be the endpoint of the evolution of metal-free massive stars (VHM). In the heavy seeds scenarios, MBHs form in the centres of high-redshift gas-rich haloes where angular momentum losses are efficient. KBD explore a model where angular momentum is shed via turbulent viscosity, in all haloes with efficient molecular hydrogen cooling. This seed formation scenario is very efficient, and predicts that seeds are widespread, forming in haloes as small as a few times $10^5\,M_\odot$, provided that the total angular momentum of the halo is small enough. BVR explore a different scenario where angular momentum is transported via runaway gravitational instabilities ('bars within bars'). BVR envisage that the process would be more effective in haloes with efficient atomic cooling, that is with virial temperature $T_{\rm vir} \gtrsim 10^4$K, and mass $M_{\rm h} \gtrsim 10^8\,M_\odot$. MBH seeds are therefore much rarer in the BVR model. BVR envisage that the process of MBH formation stops when gas is sufficiently metal enriched. Given the uncertainties in the efficiency in spreading metals, we consider here two scenarios, one in which star formation exerts a high level of feedback and ensures a rapid metal enrichment (BVRhf), one in which feedback is milder and haloes remain metal free for longer (BVRlf). In the former case MBH formation ceases at $z \approx 15$, in the latter at $z \approx 18$.

We have shown that, in all considered models, MBHB coalescences do not produce a stochastic GW background, but rather, a set of individual resolved events. A large fraction (depending on models) of coalescences will be directly observable by *LISA*, and on the basis of the detection rate, constraints can be put on the MBH formation process. Detection of several hundreds events in 3 yr will be the sign of efficient formation of heavy MBH seeds in a large fraction of high-redshift haloes (KBD).

At the other extreme, a low event rate, about few tens in 3 yr, is peculiar in scenarios where either the seeds are light, and many coalescences do not fall into the *LISA* band, or seeds are massive, but rare, as envisioned by, for example, BVR (see also Lodato & Natarajan). In this case a decisive diagnostic is provided by the mass distribution of detected events. In the light-seed scenario, the mass distribution of observed binaries extend to $\sim 10^3\,M_\odot$, while there are no sources with mass below $10^4\,M_\odot$ in the high-seed scenario. Finally, we have shown that a further, helpful diagnostic of MBH models lies in the distribution of the mass ratios in binary coalescences. While heavy seed models predicted that most of the detected events involve equal-mass binaries, in the case of light seeds, mass ratios are equally distributed in the mass ratio range 0.1–1.

Should the early black hole population be dominated by massive systems (e.g. KBD), the GW signal can be accompanied by an electromagnetic counterpart (EM; Milosavljević & Phinney 2005; Dotti et al. 2006b; Kocsis et al. 2006), in principle detectable by future high-sensitivity X-ray telescopes (e.g. XEUS[1]). The identification of an EM counterpart would have crucial implications for cosmology. *LISA* sources could then be used as 'standard sirens' (Schutz 1986) to estimate fundamental cosmological parameters (Schutz 2002; Holz & Hughes 2005), providing constraints complementary to cosmic microwave background experiments, and supernovae search experiments.

We note, however, that from the astrophysical point of view, even in absence of EM counterparts, by adopting the standard *Wilkinson Microwave Anisotropy Probe* cosmological parameters (Spergel et al. 2003) the redshift of the merging MBHs will be known with the same precision as most sources observed in electromagnetic bands.

In conclusion, concerning the detection of low-frequency GWs, MBHBs are certainly one of the major targets for a mission as *LISA*. On the astrophysical ground, *LISA* will be a unique probe of the formation, accretion and merger of MBHs along the *entire* cosmic history of galactic structures.

ACKNOWLEDGMENTS

We would like to thank A. Vecchio for helpful discussions and comments on our manuscript. This research was supported in part by the National Science Foundation under grant no. PHY99-07949.

[1] www.rssd.esa.int/index.php?project=XEUS

REFERENCES

Begelman M. C., Blandford R. D., Rees M. J., 1980, Nat, 287, 307
Begelman M. C., Volonteri M., Rees M. J., 2006, MNRAS, 370, 289 (BVR)
Bender P., 2003, Class. Quantum Gravity, 20, 301
Bender P. et al., 1994, *LISA*, Laser Interferometer Space Antenna for Gravitational Wave Measurements: ESA Assessment Study Report
Bullock J. S., Kolatt T. S., Sigad Y., Somerville R. S., Kravtsov A. V., Klypin A. A., Primack J. R., Dekel A., 2001, MNRAS, 321, 559
Cornish N. J., 2003, online-only reference (gr-qc/0304020)
Dotti M., Colpi M., Haardt F., 2006a, MNRAS, 367, 103
Dotti M., Salvaterra R., Sesana A., Colpi M., Haardt F., 2006b, MNRAS, 372, 869
Escala A., Larson R. B., Coppi P. S., Mardones D., 2005, ApJ, 607, 765
Fan X. et al., 2001, AJ, 122, 2833
Farmer A. J., Phinney E. S., 2003, MNRAS, 346, 1197
Flanagan E. E., Hughes S. A., 1998, Phys. Rev. D, 57, 4535
Haehnelt M. G., 1994, MNRAS, 269, 199
Haiman Z., Loeb A., 2001, ApJ, 552, 459
Holz D. E., Hughes S. A., 2005, ApJ, 629, 15
Hopkins P. F., Hernquist L., Cox T. J., Di Matteo T., Robertson B., Springel V., 2005, ApJ, 632, 81
Hughes S. A., 2002, MNRAS, 331, 805
Jaffe A. H., Backer D. C., 2003, ApJ, 583, 616
Kazantzidis S. et al., 2005, ApJ, 623, 67
Kocsis B., Frei Z., Haiman Z., Menou K., 2006, ApJ, 637, 27
Koushiappas S. M., Zentner A. R., 2006, ApJ, 639, 7
Koushiappas S. M., Bullock J. S., Dekel A., 2004, MNRAS, 354, 292 (KBD)
Lodato G., Natarajan P., 2006, MNRAS, 371, 1813
Madau P., Rees M. J., 2001, ApJ, 551, L27
Magorrian J. et al., 1998, AJ, 115, 2285
Mayer L., Kazantzidis S., Madau P., Colpi M., Quinn T., Wadsley J., 2007, in Aschenbach B., Burwitz V., Hasinger G., Leibundgut B., eds, Conf. Proc. Relativistic Astrophysics and Cosmology – Einstein's Legacy. ESO Astrophysics Symposia, in press
Milosavljević M., Phinney E. S., 2005, ApJ, 622, L93
Nelemans G., Yungelson L. R., Portegies-Zwart S. F., 2001, A&A, 375, 890
Quinlan G. D., 1996, New Astron., 1, 35
Schutz B. F., 1986, Nat, 323, 310
Schutz B. F., 2002, in Gilfanov M., Sunyaev R., Churazov E., eds, MPA/ESO Conf. Proc., Proceedings of the conference 'Lighthouses of the Universe: The Most Luminous Celestial Objects and Their Use for Cosmology', Springer, Berlin, p. 207
Sesana A., Haardt F., Madau P., Volonteri M., 2004, ApJ, 611, 623
Sesana A., Haardt F., Madau P., Volonteri M., 2005, ApJ, 623, 23
Shlosman I., Frank J., Begelman M. C., 1989, Nat, 338, 45
Spergel D. N. et al., 2003, ApJS, 148, 175
Thorne K. S., 1987, in Hawking S., Israel W., eds, 300 Years of Gravitation. Cambridge Univ. Press, Cambridge, p. 330
van den Bosch F. C., Abel T., Croft R. A. C., Hernquist L., White S. D. M., 2002, ApJ, 576, 21
Volonteri M., Rees M. J., 2006, ApJ, 650, 669
Volonteri M., Haardt F., Madau P., 2003a, ApJ, 582, 599 (VHM)
Volonteri M., Madau P., Haardt F., 2003b, ApJ, 593, 661
Volonteri M., Salvaterra R., Haardt F., 2006, MNRAS, 373, 121
Wyithe J. S. B., Loeb A., 2003, ApJ, 590, 691

This paper has been typeset from a TEX/LATEX file prepared by the author.